Experimental Determination of the Dynamics of a Mooring System

Edward C. Kern Jr.* and Jerome H. Milgram†
Massachusetts Institute of Technology, Cambridge, Mass.
and
Walter B. Lincoln‡
U. S. Coast Guard Research and Development Center, Groton, Conn.

A moored body system consists of an anchor, a mooring line, and the moored body itself. If the mechanics of the moored body and the mooring line are known, the motions of the system in the sea and the associated forces can be determined. Most past work on the mechanics of mooring lines has been oriented toward the development of mathematical models for their mechanics. If only the body motions, the forces in the body, and the connection between body and line are to be found, knowledge of all of the mechanics of the line is not necessary. The only required information about the mooring line is the relations between the forces and motions of the termination of the line attached to the moored body. To solve the problem of body motions and forces, an alternative to a mathematical model for the mooring line is a catalog of relations between line termination forces and motions for various mooring line geometries and current distributions. This paper sets out these ideas and reports the results of an experimental program for determining the relations between mooring line endpoint motions and forces for three different lines having different diameters and weights, but otherwise deployed in identical mooring geometries. The experiments were carried out in the absence of a current so as to have the most straightforward situation possible for the first experiments of this type which have ever been done. It was found that the relationship between mooring line endpoint forces and motions could be well approximated by linear relations, so that the concepts of impedances and admittances could be used.

Introduction

DURING the past 10 years, extensive work has been devoted to the development of computer-oriented mathematical models to simulate and predict the static and dynamic characteristics of mooring systems. This work has been done by a variety of investigators using a variety of approximate dynamical cable equations and a variety of methods of numerical solution. As a result, different mathematical models can be expected to give different predictions for the same physical situation!

Dillon[1] gave a description of 16 different computer-based mathematical models for simulating and predicting mooring system mechanics, and his list was not exhaustive. Even more mathematical models have been developed since the writing of Dillion's report.

All of the mathematical models require some means of specifying the hydrodynamic characteristics of the mooring line, such as added mass and damping that may have both linear and nonlinear components. Dillon has pointed out that some of the models exhibit strong sensitivity to the choice of these coefficients. Since the coefficients are never known precisely, the utility of such models is in doubt. Furthermore, there seem to have been no comparisons between full-scale mooring system dynamics and the dynamics predicted for the actual system by the mathematical models. Even model test comparisons are scanty and incomplete.

For many applications, all of the forces and motions of the entire cable do not have to be known. For example, if the motions of a moored body in a seaway are to be predicted, only the forces and moments exerted by the cable termination on the body need to be known in order to solve the equations of motion of the body. For cables with negligible bending stiffness, the moments are simple geometrical functions of the forces, so that only the cable termination forces need to be known. The unsteady forces of the cable termination on the body are due to both wave forces on the entire cable and motions of the cable termination. Usually the former are negligible in comparison to the latter, so that, for a particular current and mean configuration of the cable, the cable forces on the body are determined by the motions of the cable termination. Breslin[2] has given the formulation for the equations of motion of a moored body due to a sinusoidal externally applied force when the hydrodynamic forces and the cable termination forces on the body are linear functions of body motion. For the linearized case, the frequency-dependent forces exerted by the cable termination per unit amplitude of termination motion can be thought of as cable termination "impedances." The force in the direction of the motion is a "direct impedance," and the forces in the other directions are "cross impedances."

When the relationship between cable termination force and motion is nonlinear, there is still a unique relationship between the force and motion. Whereas the frequency domain mathematics involve only linear algebra in the linear case, the nonlinear case would require use of either equivalent linearization or (for more accuracy) a Volterra functional series such as has been used in other hydrodynamic problems by Lee[3] and O'Dea.[4] It is likely that accurate results almost always could be obtained by truncating the Volterra functional series after third-order terms, since the salient nonlinear force is the hydrodynamic damping.

Determination of the impedances of a particular cable configuration by use of one of the mathematical models for cable dynamics naturally requires a mathematical solution for the entire cable. However, an entirely different approach can be used to determine cable termination impedances, namely, experimental measurement. Whereas determination of the dynamics of an entire cable by a full-scale field experiment would be an enormous task, experimental determination of the termination impedances requires measurement of only the

Received Jan. 24, 1977; revision received June 16, 1977.
Index category: Marine Mooring Systems and Cable Mechanics.
*Staff Member, Lincoln Laboratory.
†Professor, Department of Ocean Engineering.
‡Ocean Engineer.

termination forces and motions, with subsequent processing of these data.

If a data base of termination impedances as functions of cable mechanical characteristics, current distribution, and mooring system geometry were developed, the determination of the termination impedances for an arbitrary mooring system could be found by interpolation or extrapolation on the data base. Knowledge of the termination impedances for a mooring system would permit a prediction of moored system performance without involving any of the uncertainties presently associated with the mathematical models of cable dynamics.

The experiments reported here were done for two purposes. The first was to determine the feasibility and degree of difficulty of making cable termination force and motion measurements in the field along with subsequent analysis of these data to determine the impedances. The second was to obtain actual field data of cable termination forces and motions in a dynamic situation which then would be available for comparison with mathematical model predictions.

Conceptual Framework for Predicting Motions of a Moored Body Using Mooring Line Termination Admittances

Let x be the six-component vector for the linear and angular displacements of a moored body measured at the point of attachment of the mooring line to the body, and let m be its generalized mass matrix with respect to this measurement point. Any six-component vector for three forces and three moments will be denoted by f and will be called a force. The sea state will be denoted abstractly by the symbol s. Then the dynamic equations of motion of the moored body can be written as

$$m\frac{d^2x}{dt^2} = f_b(x,s) + f_c(x,s) \tag{1}$$

where f_b is the force of the water on the body, and f_c is the force of the mooring line (cable) termination on the body. The symbol $f(x,s)$ is to be interpreted as meaning that the force at any time is given as a functional on the past history of the motion and the sea state.

We shall assume here that the force of the cable on the body can be decomposed as follows:

$$f_c(x,s) = f_{sc}(s) + f_{xc}(x) \tag{2}$$

where f_{sc} is the force of the cable termination on the body due to wave forces on the cable and depends only on s, whereas f_{xc} is the force of the cable termination on the body due to motion of the cable termination and depends only on x. We believe that the prediction of moored body motions from a catalog of mooring system termination admittances or impedances will be practical only if such a decomposition is possible. If the wave forces on the cable have a significant effect on body motion, a catalog of transfer functions from sea state to f_{sc} also would be needed, but making such a catalog is just as feasible as making a catalog of admittances. However, if the additive decomposition given by Eq. (2) is not an accurate approximation, the relationship between cable termination force due to body motion and the body motion would be different for each sea state, and the experimental determination of enough of these relationships would be impossible from the practical point of view. We do point out here that most existing mathematical models for predicting moored system performance neglect wave forces on the cable altogether, so that, in effect, the decomposition given by Eq. (2) is carried to an extreme! An exception is the model of Goodman and Breslin[5] which accounts for wave forces in the form of the decomposition given by Eq. (2).

For simplicity in our presentation here, we shall write f_b in the form

$$f_b(x,s) = f_{sb}(s) + f_{xb}^{(s)}(x) \tag{3}$$

where f_{sb} would be the force of the water on the body due to the sea state if the body were motionless. $f_{xb}^{(s)}(x)$ is to be interpreted as a functional on (x), with s being a parameter. In the linear approximation for the fluid forces on the body, f_{xb} would be independent of (s).

Then, denoting the left-hand side of Eq. (1) by $f_{xm}(x)$, we can write that equation as

$$[f_{xm} - f_{xc} - f_{xb}^{(s)}](x) = [f_{sc}(s) + f_{sb}(s)] \tag{4}$$

If the functional operation of the left-hand side of Eq. (4) were known, its inverse could be determined, and the body motion could be written as

$$x = [f_{xm} - f_{xc} - f_{xb}^{(s)}]^{-1}[f_{sc}(s) + f_{sb}(s)] \tag{5}$$

The special, and possibly most useful, case when forces are linear and independent functionals of the sea state and the body motions will be described here. The seas will be considered to be unidirectional, so that the sea state is described by the surface elevation $y(t)$ measured at the mean position of the body on the free surface. For the linear case, the functionals f are convolution integrals, and by taking the Fourier transform of Eq. (4) an equation in the frequency domain is obtained which involves only matrix multiplication of complex numbers:

$$[-m\omega^2 - F_{xc}(\omega) - F_{xb}(\omega)][X(\omega)] = [F_{sc}(\omega) + F_{sb}(\omega)][Y(\omega)] \tag{6}$$

In this equation, ω is the radian frequency, F_{xc} is the impedance matrix of the upper termination of the cable, X is the Fourier transform of the body motion, F_{sc} is the transfer function from wave elevation to force exerted by the cable termination due to wave forces on the cable, F_{sb} is the transfer function from wave elevation to force exerted on the body by the waves, and Y is the Fourier transform of the surface elevation. F_{xb} is the frequency-dependent complex matrix relating fluid forces due to body motions to those motions. It often is decomposed as follows:

$$F_{xb}(\omega) = \omega^2 M_a(\omega) - i\omega B(\omega) - K \tag{7}$$

where M_a, B, and K are real, and M_a is the added mass matrix, B is the damping matrix, and K is the hydrostatic spring constant matrix. In this notation, the motion is given as

$$X = [K - \omega^2(m + M_a(\omega)) - i\omega B(\omega) - F_{xc}(\omega)]^{-1} \times [F_{sc}(\omega) + F_{sb}(\omega)][Y(\omega)] \tag{8}$$

Methods of determining the wave- and motion-induced fluid forces on the body f_{sb} and f_{xb} have received much attention, and in general predictions of these forces can be made. Reviews on various aspects of these methods have been given by Wehausen,[6] Hogben,[7] and Milgram.[8]

This paper is addressed toward the feasibility of determining f_{xc} experimentally. This was done by applying known transient forces to the end of a cable and determining the resulting motions. Since the motion was in a plane and the cables had negligible bending stiffness, the impedance matrices were 2×2. The analysis of the experimental data was found to be most convenient if the admittance matrices were found, these being the inverses of the impedance matrices.

No work has been done yet on the determination of f_{sc} for actual cables. However, if it is found to be convenient to

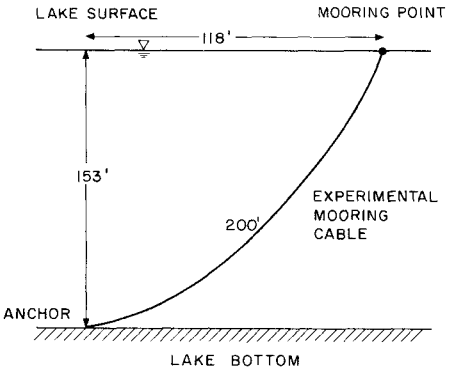

Fig. 1 Basic experimental configuration.

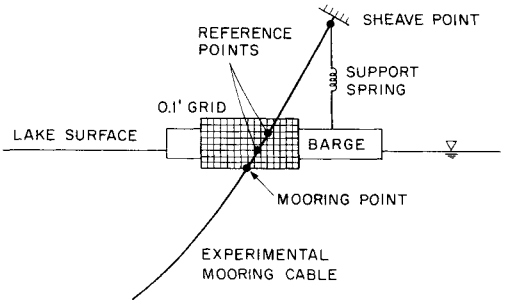

Fig. 2 Support and measurement system details.

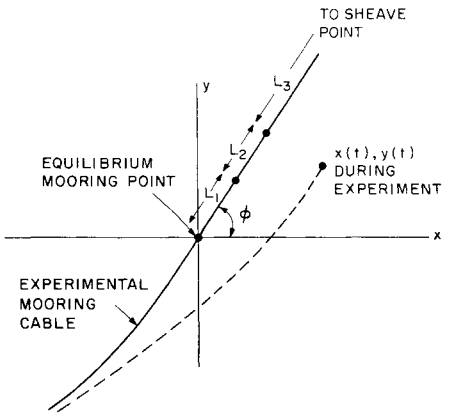

Fig. 3 Coordinate system.

catalog f_{xc} or related nonlinear measures of force relationships as functions of cable geometry, it will be just as convenient to catalog similar measures of f_{sc} as functions of the same geometrical variables. Field determination of f_{sc} could be made from simultaneous measurements of waves and the forces applied by the fixed upper end of a cable on a dynamometer due to wave forces on the cable.

Experiments

Site selection for these experiments was based on the necessity both to utilize a large model for the proper scaling of Reynolds number effects and also to maintain reasonable control over environmental influences on the results. This criterion was met by Lake Winnepesaukee in central New Hampshire, where a reasonably protected location with a water depth of 153 ft was available. Figure 1 gives an overview of the configuration of the experimental mooring.

The data sought in these experiments were the transient forces applied to the upper ends of various mooring lines and their respective motions. As illustrated in Fig. 2, the upper end of an experimental mooring line (the mooring point) was connected to a support spring through a sheave. During an experimental run, either a supplemental vertical or horizontal force was applied to the mooring point and the system allowed to come to rest in a new equilibrium position. When the supplemental force was removed suddenly, the mooring point returned to the original equilibrium position in a transient manner. These motions were recorded on motion pictures with a nominal frame rate of 16 frames/sec.

The trajectory of the mooring point (Figs. 1 and 2) during the transient was determined by recording the coordinates, in the coordinate system shown in Fig. 3, of two reference points on the support string between the mooring point and the sheave. The mooring point location, whose trajectories were both above and below the water surface, was determined by linear extrapolation from these reference points. A means of easily determining the reference point coordinates from the motion pictures was provided through the use of a background grid of 0.1-ft squares. Support system force data were calculated from the known spring constant of the support spring and from its extension as determined by the radial distance from the sheave point to the mooring point (Fig. 2). Timing information was provided by means of a clock with a sweep second hand mounted on the background grid so that it appeared in the pictures.

The support system and background grid were carried on a barge that was held stationary by a taut four-legged mooring system. A small boat anchored nearby carried the

Table 1 Experimental details

	3/16-in.-diam wire rope	5/8-in.-diam polyester, double braid	1 5/16-in.-diam polyester, double braid
Mooring point	10.7	5.45	30.60
Measured static tension, lb	74.78	76.32	80.32
Static angle, deg			
Support spring constant, lb/ft	3.04	8.30	34.27
Cable length, ft	201	201	201
Water depth, ft	153	153	153
Horizontal anchor to mooring point distance, ft	118	118	118
Sheave coordinates			
X, ft	3.84	3.15	2.14
Y, ft	14.11	12.94	13.24
Cable weight, lb/ft	0.062	0.103	0.56
Specific gravity of cable material	7.84	1.38	1.38
Net weight in fresh water, lb/ft	0.0541	0.0303	0.1542

cameraman. Experiments were conducted during early morning hours to minimize the most significant environmental influences: incident wind waves and boat wakes.

The physical properties of the experimental mooring systems tested are given in Table 1. These were chosen to represent a broad range of cable diameters and weights. In all cases, the water depth was 153 ft, and the horizontal extent of the mooring was 118 ft. A catenary of these dimensions which is tangent to the bottom has a length of 214 ft. All experimental cables had a length of 201 ft, chosen less than 214 ft to avoid the complexity of a varying length of cable lying on the bottom.

The variation in mooring point static angles listed in Table 1 is a matter of concern. If the static shapes were catenaries, they all should be the same. The angles were measured between the support string and the horizontal axis of the background grid. The 1.54-deg difference between the endpoint angles of the 3/16-in.-diam wire rope and the 5/8-in.-diam polyester line could be due to trim of the raft or misalignment of the background grid. However, the 4-deg difference between the 1 5/16-in.-diam polyester line endpoint angle and that of the other lines is too large for these reasons to apply. It seems likely that either the anchor dragged or air entrapped in the line altered its static configuration. For comparing the experimental results with any mathematical model, it would seem appropriate to do the mathematical analysis for the 1 5/16-in.-diam line with the horizontal distance from the mooring point to the anchor reduced from the nominal value of 118 ft so as to achieve the measured static angle of 80.32 deg. Naturally, mooring point impedances and admittances will depend on the static cable configuration.

Data Smoothing and Averaging

The motion data response recorded on movie film consisted of the coordinates of the reference points as shown in Fig. 2. These values were read, frame by frame, and punched onto computer cards in units of 0.01 ft, with an estimated error bound of ± 0.01 ft.

The mooring point data then were smoothed using a least-squares curve-fitting technique with a set of nonorthogonal functions (Table 2) chosen to give a rapidly convergent series representation of the transient motion. This procedure was multipurposed. First, it provided a convenient means for handling the data using a small number of coefficients (less than six) rather than several hundred measured values. Second, the least-squares procedure filtered out high-frequency oscillations believed to have resulted from short wind wave excitation. Finally, the analytic representation of the data afforded the opportunity to take Fourier transforms from the time domain to the frequency domain analytically. This facilitated inclusion of the semi-infinite periods prior to and subsequent to the recorded transient data. The coefficients c_n for each of the time functions considered in this analysis are given in Table 3. This allows the interested reader to reconstruct the smoothed force and motion time functions. Figure 4 gives an example of measured data and the results of application of the curve fitting process to it.

For each type of cable tested, both horizontal and vertical excitation experiments were conducted with varying initial displacement. To determine an average response, the individual smoothed response records first were summed, and the result then was normalized so that the initial value was unity. This procedure weighted each function in proportion to its initial amplitude. The averaging was done at 0.25-sec intervals using the curve-fit approximations to the raw data. Finally, the 0.25-sec interval record was fit by the same procedure. The normalization of the vertical response during a horizontal excitation experiment was that of scaling by the same factors as for the response in the direction of excitation. In Table 4, where these coefficients are tabulated, the initial motion in the direction of the excitation always will equal unity, and the other motion generally will be smaller for the horizontal supplemental force tests and larger for the vertical

Table 2 Curve-fitting functions and their transforms[a]

Function	Transform
$f_1(t) = \begin{cases} 1 & \text{for Table 3} \\ e^{-t/T} & \text{for Table 4} \end{cases}$	$F_1(\omega) = 1/(i\omega + 1/T)$ for Table 4 [Note that transform assumes $f_1(t) \neq 0$ for $t > T$]
$f_2(t) = e^{-4.91\,t/T}$	$F_2(\omega) = 1/(i\omega + 4.91\,t/T)$ (Note that above also applies here)
$f_n(t) = \sin(\pi k t/T)$ $n = 2, 3, \ldots$ $k \equiv n-2$	$F_n(\omega) = \pi k \dfrac{1-\cos(\pi k)e^{i\omega T}}{[\pi(k/T)]^2 - \omega^2}$

[a] Experimental data were recorded from $t = 0$ until $t = T$.

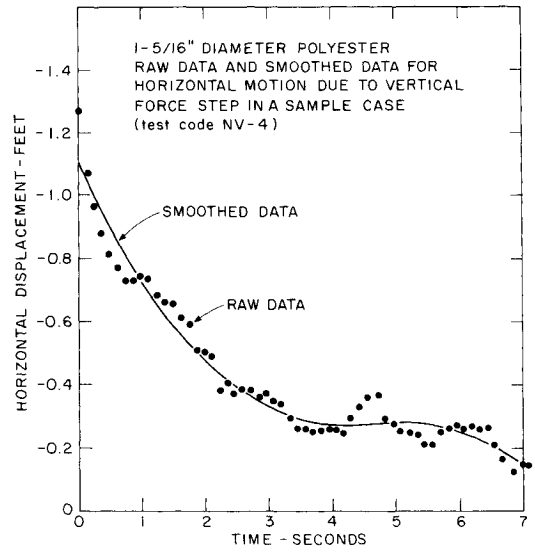

Fig. 4 Example of curve-fitting process.

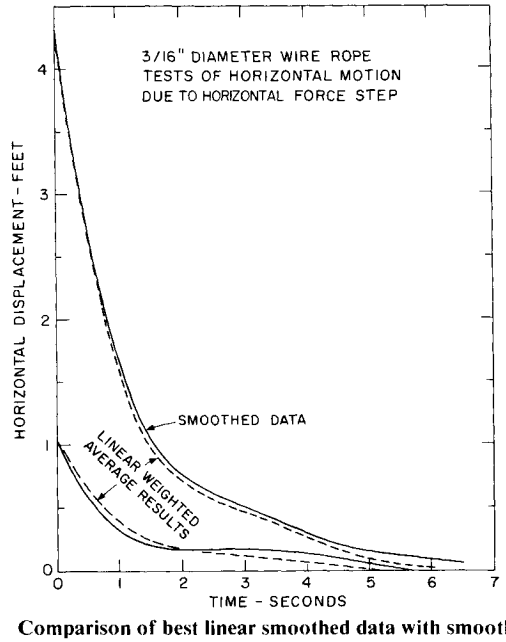

Fig. 5 Comparison of best linear smoothed data with smoothed data records from two individual transient motion tests.

Table 3 Curve-fitting coefficients for individual tests[a]

Material test type	Run number test duration, sec		X motion, ft	Y motion, ft
⅝-in.-diam polyester, horizontal	DH – 1 6.667	c_1	–0.355 E – 01	0.523 E – 02
		c_2	0.115 E 01	–0.100 E 00
		c_3	0.153 E 00	–0.445 E – 01
		c_4	0.294 E – 02	–0.312 E – 01
		c_5	0.146 E – 01	–0.174 E – 01
		c_6	–0.389 E – 01	0.111 E – 02
⅝-in.-diam polyester, horizontal	DH – 2 6.111		0.122 E 00	–0.743 E – 01
			0.184 E 01	–0.157 E 00
			0.272 E 00	–0.221 E – 01
			0.392 E – 01	–0.387 E – 01
			0.329 E – 01	–0.375 E – 02
			–0.170 E – 01	–0.135 E – 01
⅝-in.-diam polyester, vertical	DV – 7 6.605		0.436 E – 02	0.447 E – 01
			–0.109 E 01	0.556 E 00
			–0.179 E – 01	–0.146 E – 01
			–0.820 E – 02	–0.185 E – 01
			0.118 E – 01	–0.241 E – 01
			–0.190 E – 01	–0.103 E – 01
⅝-in.-diam polyester, vertical	DV – 8 6.605		0.100 E – 01	0.356 E – 01
			–0.155 E 01	0.940 E 00
			–0.192 E – 01	0.290 E – 01
			–0.427 E – 01	–0.329 E – 01
			0.448 E – 01	–0.366 E – 01
			0.251 E – 01	–0.241 E – 01
⅝-in.-diam polyester, vertical	DV – 9 4.568		0.169 E – 01	0.497 E – 01
			–0.207 E – 01	0.109 E 01
			–0.306 E 00	0.600 E – 01
			–0.116 E 00	0.315 E – 01
			–0.327 E – 01	0.140 E – 01
			0.821 E – 03	0.119 E – 01
⅝-in.-diam wire rope, horizontal	WH – 2 5.064		–0.186 E – 01	0.643 E – 01
			0.106 E 01	–0.231 E 00
			0.802 E – 01	–0.603 E – 02
			–0.926 E – 01	0.172 E – 01
			–0.827 E – 02	...
			–0.358 E – 02	...
⅝-in.-diam wire rope, horizontal	WH – 3 7.244		–0.113 E 00	0.254 E – 01
			0.434 E 01	–0.266 E 00
			0.602 E – 02	–0.102 E 00
			–0.231 E 00	–0.283 E – 01
			–0.123 E 00	–0.606 E – 02
			–0.101 E 00	0.141 E – 01
⅝-in.-diam wire rope, horizontal	WH – 13 7.048		–0.123 E 00	–0.589 E – 02
			0.433 E 01	–0.175 E 00
			–0.121 E 00	–0.943 E – 01
			–0.188 E 00	–0.458 E – 01
			–0.146 E 00	–0.375 E – 02
			–0.877 E – 01	0.654 E – 02
⅝-in.-diam wire rope, vertical	WV – 9 5.060		–0.118 E – 01	0.545 E – 01
			–0.883 E 00	0.154 E 01
			0.228 E – 01	–0.158 E 00
			0.248 E – 01	–0.955 E – 01
			0.569 E – 01	–0.415 E – 01
			0.127 E – 01	0.170 E – 02
⅝-in.-diam wire rope, vertical	WV – 11 6.988		0.370 E – 01	–0.143 E – 01
			–0.130 E 01	0.205 E 01
			–0.101 E 00	–0.113 E 00
			0.381 E – 01	–0.172 E 00
			–0.122 E – 01	–0.771 E – 01
			0.609 E – 01	–0.445 E – 01
⅝-in.-diam wire rope, vertical	WV – 16 1.687		–0.408 E – 02	–0.238 E – 02
			–0.336 E 00	0.348 E 00
			–0.464 E – 01	0.526 E – 01
			–0.262 E – 02	0.534 E – 01
			–0.647 E – 02	0.221 E – 01
			0.862 E – 02	...
1 5/16-in.-diam polyester, vertical	NV – 3 6.258		–0.267 E 00	0.885 E – 01
			–0.754 E 00	0.562 E 00
			0.755 E – 01	0.211 E – 01
			0.256 E – 01	–0.774 E – 01
			0.261 E – 01	–0.308 E – 01
			0.134 E – 03	–0.567 E – 01
1 5/16-in.-diam polyester, vertical	NV – 4 7.055		–0.132 E 00	0.549 E – 01
			–0.978 E 00	0.639 E 00
			–0.122 E 00	0.101 E 00
			–0.134 E – 02	–0.635 E – 01
			–0.494 E – 01	–0.278 E – 02
			–0.314 E – 02	–0.371 E – 01
1 5/16-in.-diam polyester, vertical	NV – 5 5.153		–0.298 E 00	0.145 E 00
			–0.131 E 01	0.860 E 00
			–0.155 E 00	0.167 E – 01
			–0.283 E – 01	–0.812 E – 01
			–0.563 E – 01	–0.271 E – 01
			–0.280 E – 01	–0.410 E – 01
1 5/16-in.-diam polyester, horizontal	NH – 5 10.536		0.955 E – 01	–0.947 E – 02
			0.469 E 01	0.350 E – 01
			–0.241 E – 02	–0.107 E 00
			–0.121 E 00	–0.623 E – 01
			–0.844 E – 01	–0.448 E – 01
			–0.739 E – 01	–0.253 E – 01
1 5/16-in.-diam polyester, horizontal	NH – 6 13.512		–0.281 E – 01	0.658 E – 01
			0.552 E 01	0.224 E 00
			–0.434 E – 01	–0.688 E – 01
			–0.317 E 00	–0.883 E – 01
			–0.108 E 00	–0.538 E – 01
			–0.116 E 00	–0.554 E – 01
1 5/16-in.-diam polyester, horizontal	NH – 7 12.917		0.316 E – 01	–0.584 E – 01
			0.548 E 01	0.193 E 00
			–0.646 E – 01	–0.715 E – 01
			–0.161 E 00	–0.105 E 00
			–0.132 E 00	–0.431 E – 01
			–0.104 E 00	–0.492 E – 01

[a] These coefficients permit reconstruction of the smoothed motion functions by use of the functions given in Table 2. Smoothed force functions can be obtained by the geometry of the support and cable end specified by the motion and the data in Figs. 1 and 2 and Table 1.

tests. Similarly, the sum of the force records was scaled by the same factor. An indication of the success of these procedures may be seen in the example shown in Fig. 5, where average curves, scaled to have the proper initial value, are compared to some individual smoothed records.

Mooring Line Transfer Functions

With the motion response for each kind of experiment in coefficient form, the corresponding force records were generated at 0.25-sec intervals using the known characteristics of the spring support system. These records then were curve-fit to facilitate handling and transforming to the frequency domain. These force coefficients, tabulated in Table 4, correspond to the motion coefficients and reflect the forces experienced during a transient response of unit initial value. As shown by Fig. 6, the force records have discontinuities at time zero when the external "excitation" force is removed suddenly. The corresponding displacement record has a nearly discontinuous slope, which indicates that inertia may not play a dominant direct role in the response.

Fourier transforming these records is a straightforward procedure involving the summation of the transforms for the analytically described components of the time domain data. For $t<0$, the transform of a step function is used, and for $t>0$, the transforms of the curve-fitting functions are used with weighting equal to their weighting in the time domain. In the time domain, the motion and force responses are assumed to be zero for $t>T$, and the curve-fitting is carried out only over the range $0<t<T$. Because a small discontinuity in the time domain response representation with the fitting functions generally results if one assumes zero motion and force

Table 4 Best linear average force and motion curve-fitting coefficients

Material test duration	External excitation, lb	X motion, ft	Y motion, ft	X force, lb	Y force, lb
1 5/16-in.-diam polyester, 13.5 sec	Horizontal, 2.96	+0.554E−03	−0.775E−02	−0.603E−03	+0.153E 00
		+0.992E 00	+0.218E−01	−0.223E+01	−0.461E+01
		−0.183E−01	−0.597E−02	+0.413E−01	+0.231E 00
		−0.481E−01	−0.142E−01	+0.106E+00	+0.591E 00
		−0.246E−01	0.0	+0.573E−01	+0.481E−01
		−0.216E−01	0.0	+0.499E−01	+0.511E−01
1 5/16-in.-diam polyester, 6.5 sec	Vertical, 15.83	−0.722E 00	+0.535E 00	−0.424E 00	−0.138E+02
		−0.825E 00	+0.448E 00	−0.145E+01	−0.679E+01
		+0.100E 00	−0.139E 00	+0.563E 00	+0.386E+01
		+0.490E−01	−0.113E 00	+0.680E 00	+0.319E+01
		+0.123E−01	−0.671E−01	+0.484E 00	+0.198E+01
		−0.135E−01	−0.456E−01	+0.408E 00	+0.148E+01
⅜-in.-diam polyester, 6.0 sec	Horizontal, 0.42	+0.183E 00	−0.781E−01	−0.119E 00	+0.273E 00
		+0.817E 00	−0.320E−01	−0.283E 00	−0.948E 00
		+0.703E−01	−0.124E−02	0.0	−0.124E 00
		+0.746E−02	−0.178E−01	0.0	+0.113E 00
		+0.352E−02	0.0	0.0	−0.154E−01
		−0.171E−01	0.0	0.0	+0.223E−01
⅜-in.-diam polyester, 6.0 sec	Vertical, 2.58	+0.472E−01	+0.206E 00	−0.396E 00	−0.177E+01
		−0.177E+01	+0.788E 00	−0.137E 00	−0.171E+01
		−0.926E−01	−0.639E−01	+0.201E 00	+0.575E 00
		−0.552E−01	−0.291E−01	+0.114E 00	+0.225E 00
		0.0	−0.312E−01	0.0	−0.595E−01
		0.0	0.0	0.0	−0.406E−01
3/16-in.-diam wire rope, 6.0	Horizontal, 1.04	+0.109E−01	−0.225E−01	−0.116E−01	+0.913E−01
		+0.989E 00	−0.411E−01	−0.695E 00	−0.423E 00
		−0.104E−01	0.0	+0.894E−02	−0.233E−01
		−0.360E−01	0.0	+0.262E−01	+0.122E−01
		−0.304E−01	0.0	+0.218E−01	0.0
3/16-in.-diam wire rope, 6.5	Vertical, 3.44	+0.351E−01	+0.339E−01	−0.328E−03	−0.534E 00
		−0.625E 00	+0.970E 00	−0.381E−01	−0.105E+01
		−0.237E−01	−0.911E−01	+0.372E−01	+0.235E 00
		+0.883E−02	−0.894E−01	+0.463E−01	+0.198E 00
		+0.184E−01	−0.416E−01	0.0	+0.904E−01
		+0.217E−01	−0.203E−01	0.0	+0.551E−01

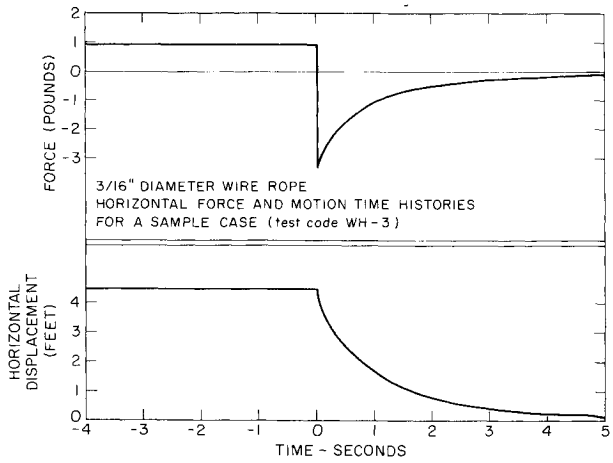

Fig. 6 Examples of overall system response.

for $t > T$, the two exponential fitting functions are considered to extend to $t = \infty$, thus permitting at worst a discontinuity of the slope of the response at $t = T$. In transforming to the frequency domain, this assumption helps remove high-frequency components that otherwise would be associated incorrectly with small step functions at $t = T$.

Transfer functions are calculated from the Fourier transforms. Because both the measured cross forces (e.g., vertical force in the horizontal string excitation experiment) and the vertical motion during horizontal experiments were small, Eq. (4) can be approximated by the simplification

$$\begin{bmatrix} T_{xx} & T_{xy} \\ T_{yx} & T_{yy} \end{bmatrix} \begin{bmatrix} \bar{F}_{xx} & 0 \\ 0 & \bar{F}_{yy} \end{bmatrix} = \begin{bmatrix} \bar{X}_x & 0 \\ \bar{Y}_x & \bar{Y}_y \end{bmatrix}$$

The transfer functions then can be calculated directly as

$$T_{xx} = \bar{X}/\bar{F}_{xx},\ T_{xy} = 0$$

$$T_{yx} = \bar{Y}_x/\bar{F}_{xx},\ T_{yy} = \bar{Y}_y/\bar{F}_{yy}$$

The transfer functions calculated using the preceding equations are shown in Fig. 7.

Discussion

We are confident that our experimental and data-reduction procedures have measured and analyzed accurately the salient motions of the cable mooring point. For these motions, the computed forces have been found with sufficient accuracy to conclude that the system is dominated by linear effects. For finer detail, however, our confidence in the results is impaired by several aspects of the experimental procedures. The control over external influences from small boat wakes and small wind waves could have been improved upon. The use of calm early-morning hours minimized these influences (especially small boat wakes) but did not eliminate the wind waves altogether, which may contribute to the small-scale, high-frequency motions that were filtered out with smoothing techniques.

From an engineering practice viewpoint, the linearity of the dominant forces is a most useful result. Confident resolution of smaller-scale motions and forces may, however, show nonlinearities. For application, such nonlinearities should be measured carefully and scaling effects considered.

In our experiments, the mooring point trajectory is believed to be accurate to within ±0.04 ft. With typical excursions several feet, this represents a satisfactory tradeoff of resolution vs time consumed reading the data from the films. The force data, however, are estimated to be accurate only

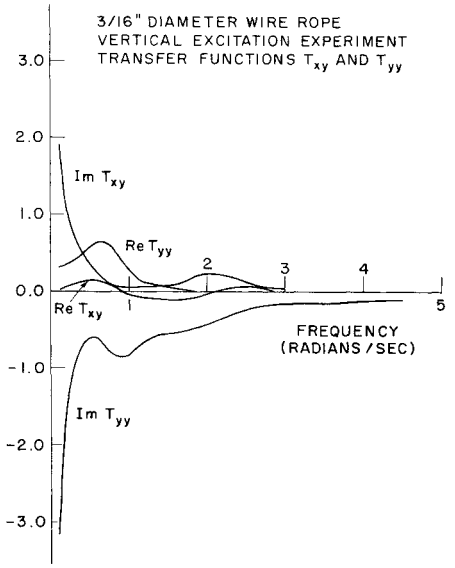

Fig. 7a Mooring point transfer functions.

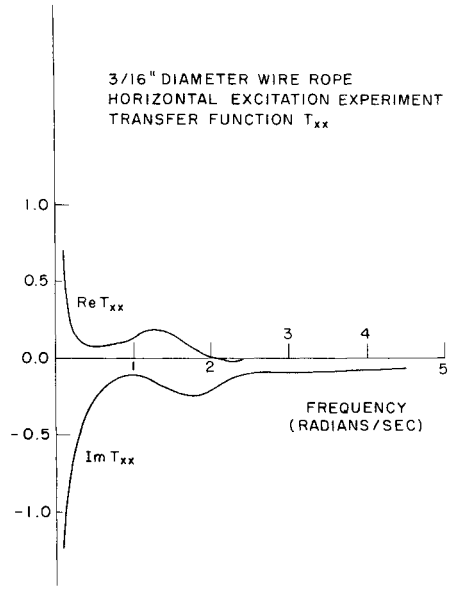

Fig. 7b Mooring point transfer functions.

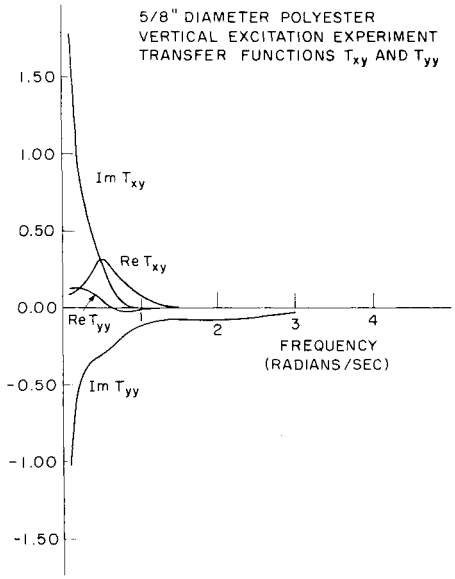

Fig. 7c Mooring point transfer functions.

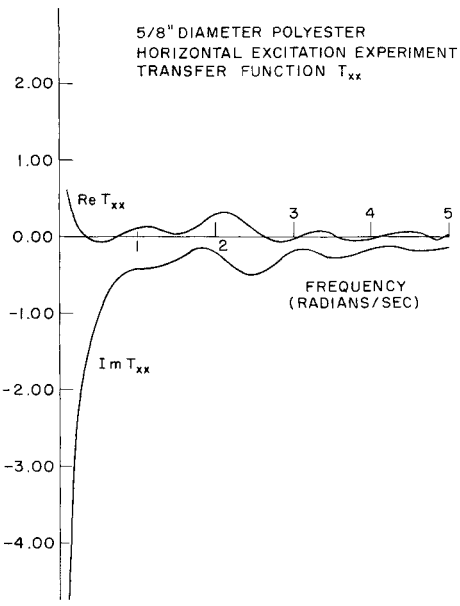

Fig. 7d Mooring point transfer functions.

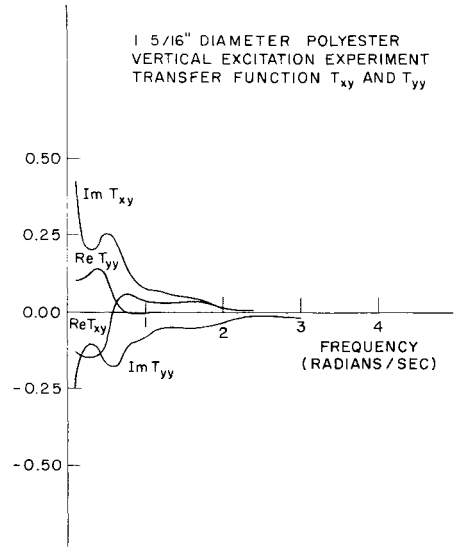

Fig. 7e Mooring point transfer functions.

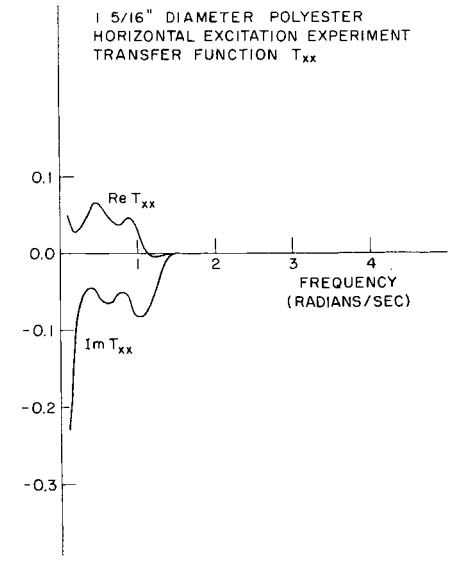

Fig. 7f Mooring point transfer functions.

within ±10%. This reflects our uncertainty regarding the support spring and the sheave location, problems with apparently simple solutions.

One quite apparent aspect of the data is that they reflect an overdamped system, since the transient motion decays without dominant oscillations. A mechanical system comprised of springs and dampers would show such characteristics. It can be shown that, if a linear force and motion relationship at the mooring point is given by

$$F = KX + C\dot{X}$$

then the transfer function corresponding to the experimentally determined ones would be given by

$$T_{xx} = (K_{xx} - i\omega C_{xx}) / (K_{xx}^2 + \omega^2 C_{xx}^2)$$

$$T_{yy} = (K_{yy} - i\omega C_{yy}) / (K_{yy}^2 + \omega^2 C_{yy}^2)$$

$$T_{xy} = (K_{xy} - i\omega C_{xy}) / T_{xx} T_{yy}$$

where ω is the radian frequency, and K_{xy} is the linear spring constant for forces in the x direction due to motions in the y direction, etc. In calculating the foregoing, use was made of the experimental result for the geometry we tested that T_{yx} is zero.

For stable and conservative systems, the real parts of the coefficients C_{ii} and K_{ii} must be positive and their imaginary parts negative. This is in agreement with nearly all of the transfer functions determined from the experimental data. The exceptions are few and small and thought to be due to experimental error. As a result, inertial effects appear to be small for these experiments.

The experimental data presented here hopefully will be of use to those working in the area of mooring system dynamics. More important, however, is the fact that it appears entirely feasible to characterize the mechanics of a cable termination by endpoint transfer functions (impedances) and to use these functions in the prediction of moored system performance.

References

[1] Dillion, D. B., "An Inventory of Current Mathematical Models of Scientific Data Gathering Moors," Hydrospace-Challenger, TR 4450-0001, Jan. 1973.

[2] Breslin, J. P., "Dynamic Forces Exerted by Oscillating Cables," *Journal of Hydronautics*, Vol. 8, Jan. 1974, pp. 19-31.

[3] Lee, C. M., "The Second Order Theory for Nonsinusoidal Oscillations of a Cylinder in a Free Surface," *Eighth ONR Symposium on Naval Hydrodynamics*, 1970.

[4] O'Dea, J. F., "Low Frequency Forces on a Body in Random Waves," Ph.D. Thesis, Dept. of Ocean Engineering, Massachusetts Inst. of Technology, 1974.

[5] Goodman, T. R. and Breslin, J. P., "Statics and Dynamics of Anchoring Cables in Waves," *Journal of Hydronautics*, Vol. 10, Oct. 1976, pp. 113-120.

[6] Wehausen, J. V., *Annual Review of Fluid Mechanics*, Vol. 3, 1971, p. 237.

[7] Hogben, N., "Fluid Loading on Offshore Structures, A State of Art Appraisal: Wave Loads," Maritime Technology, Monograph 1, 1974.

[8] Milgram, J. H., "Waves and Wave Forces," *Proceedings of BOSS '76*, Vol. 1, 1976.